

## A bifunctional nanocarrier based on amphiphilic hyperbranched polyglycerol derivatives†

Cite this: *J. Mater. Chem. B*, 2013, **1**, 3569Indah N. Kurniasih,<sup>a</sup> Hua Liang,<sup>b</sup> Sumit Kumar,<sup>c</sup> Andreas Mohr,<sup>d</sup> Sunil K. Sharma,<sup>e</sup> Jürgen P. Rabe<sup>b</sup> and Rainer Haag<sup>\*a</sup>

We here report on the synthesis of a bifunctional nanocarrier system based on amphiphilic hyperbranched polyglycerol (hPG), which is modified by introducing hydrophobic aromatic groups to the core and retaining hydrophilic groups in the shell. "Selective chemical differentiation" and chemo-enzymatic reaction strategies were used to synthesize this new core-shell type nanocarrier. The system shows an innovative bifunctional carrier capacity with both polymeric and unimolecular micelle-like transport properties. Hydrophobic guest molecules such as pyrene were encapsulated into the hydrophobic core of modified hPG *via* hydrophobic interactions as well as  $\pi$ - $\pi$  stacking, analogous to a unimolecular micelle system. A second guest molecule, which has a high affinity to the shell like Nile red, was solubilized in the outer shell of the host molecule, thus connecting the nanocarrier molecules to form aggregates. This model is confirmed by UV-Vis, fluorescence, atomic force microscopy, and dynamic light scattering, as well as release studies triggered by pH-changes and enzymes. Encapsulated guest molecules, respectively in the core and in the shell, present different controlled release profiles. The bifunctional nanocarrier system is a promising candidate for simultaneous delivery of different hydrophobic drugs for a combination therapy, e.g., in tumor treatment.

Received 15th March 2013

Accepted 16th May 2013

DOI: 10.1039/c3tb20366b

[www.rsc.org/MaterialsB](http://www.rsc.org/MaterialsB)

## Introduction

Nanocarrier systems based on amphiphilic macromolecules for drug delivery have become increasingly interesting in recent years due to the unique properties of these polymer systems, such as their enhanced permeability and retention (EPR) effect on tumor tissue<sup>1,2</sup> as well as their high aqueous solubility and biocompatibility. They help to improve therapeutic efficiency and lower toxicity by increasing drug solubility and by targeted delivery and controlled release. In particular, polymeric micelles (10 to 100 nm) composed of an amphiphilic linear block copolymer, such as a pluronic block copolymer in aqueous solution, can complex hydrophobic drugs inside their hydrophobic core by non-covalent interactions.<sup>3,4</sup> Their promising carrier properties have been explored and already

employed in clinical applications.<sup>5,6</sup> However, polymeric micelles are not very stable under varying conditions like the changes of temperature and pressure used in sterilization. They also break apart when the concentration is lower than its critical micelle concentration (CMC). Therefore the polymer concentration needs to always be kept above the CMC during application, which leads to an increase in dose and toxicity.

Alternatively, single dendrimers (*ca.* 5–20 nm), with a hydrophobic inner core and a hydrophilic shell, can form so-called "unimolecular micelles," which are stable and suitable for applications even at low polymer concentrations.<sup>7</sup> However the multi-step synthesis and purification of perfect branched structure dendrimers hinder practical usage.

Alternatively, hyperbranched polymers, synthesized by a one-pot process, combine the advantages of both polymeric micelles and unimolecular micelles in drug delivery.<sup>8</sup> Dendritic polyglycerol (DPG) architectures with controlled molecular weights, sizes, surface charges, and chemical diversity have been synthesized lately.<sup>9–11</sup> A mechanism for cellular internalization of hyperbranched polyether derivatives consisting of dye-functionalized hyperbranched polyglycerols (hPGs) with varied molecular mass and size range has been studied recently.<sup>12</sup> The results suggest that endocytotic uptake of macromolecules can be achieved above a certain molecular weight level and is suppressed for lower molecular weights. The structure-biocompatibility relationship of DPG derivatives possessing neutral, cationic, and anionic charges has also been explored by our groups.<sup>13</sup> The effect

<sup>a</sup>Institute of Chemistry and Biochemistry, Freie Universität Berlin, Takustr. 3, 14195 Berlin, Germany. E-mail: haag@chemie.fu-berlin.de; Fax: +49 30 83853357; Tel: +49 30 83852633

<sup>b</sup>Department of Physics, Humboldt-Universität zu Berlin, Newtonstr. 15, 12489 Berlin, Germany. E-mail: rabe@physik.hu-berlin.de; Fax: +49 30 20937632; Tel: +49 30 20937621

<sup>c</sup>Department of Chemistry, Deenbandhu Chhotu Ram University of Science and Technology, Murthal, India

<sup>d</sup>Division of Chemistry and Material Science, Faculty of Technology and Bionics, Rhine-Waal University of Applied Sciences, Marie Curie Straße 1, 47533 Kleve, Germany

<sup>e</sup>Department of Chemistry, University of Delhi, Delhi – 110007, India

† Electronic supplementary information (ESI) available: Experimental details and NMR, UV-Vis and fluorescent spectra. See DOI: 10.1039/c3tb20366b

of solution pH on the surface charge was studied in buffered aqueous solution between pH 4.8 and 7.4. *In vivo* results also show that the dPGs have a similar safety profile to the established linear PEG. Therefore, dPG is an ideal candidate as a new biocompatible polymer for drug delivery.<sup>11,13–15</sup> Lately, hyperbranched dendritic PG core architectures have been modified with PEG moieties. These architectures have great potential for biomedical applications.<sup>16–18</sup> Brooks *et al.* also reported the synthesis of a new class of unimolecular micelles based on hPGs that can be used as effective human serum albumin substitutes and as general drug delivery vehicles. These amphiphilic systems have also been reported to adsorb onto the human RBCs *in vitro* and to show very promising sustained drug-release characteristics *in vitro* using the drug paclitaxel, low organ accumulation, high stability with a long shelf life, and degradation under acidic conditions.<sup>16,17,19</sup> Frey *et al.* have developed linear-hyperbranched  $\alpha,\omega_n$ -telechelic block copolymers, consisting of a linear PEG block and a hPG block with a single amino moiety in the  $\alpha$ -position and subsequent attachment of biotin in this position. They have used this material subsequently for non-covalent bio-conjugation which can be achieved with or without a linear PEG-spacer.<sup>20</sup> Furthermore, Paleos *et al.* prepared functional hyperbranched polymers based on a commercially available polyether polyol and bearing protective PEG chains at their end. These PEG chains provide a protective coating for drugs and their carriers, enhance the encapsulation efficiency, and control the release of pyrene and tamoxifen.<sup>21</sup>

In many macromolecular architectures, post-polymerization modification is a powerful approach for fine tuning functional groups. Such chemical modification can be easily performed on hPG using classical hydroxyl group chemistry to change the hPG hydroxyl groups, namely, to alkynes, amines, and many others.<sup>22</sup> Unlike dendrimers, hPGs show no clearly distinguishable interior or periphery. Instead they possess two types of hydroxyl functionalities arising from linear and terminal hydroxyl units. These linear hydroxyl groups are close to the core while the terminal ones are close to the periphery of the molecule. The “selective chemical differentiation” strategy enables one to selectively modify these two types of hydroxyl groups to generate core–shell-type architectures within the hPG scaffold.<sup>22–25</sup> In recent work, we synthesized a new core–shell architecture based on hPG by attaching a mono(methoxy)polyethylene glycol (mPEG) shell either directly or through a hydrophobic biphenyl spacer to the hPG scaffold *via* “click chemistry” as a nanocarrier system. Alternatively, the hPG core was decorated with hydrophobic segments specially located around the hPG using the “selective chemical differentiation” strategy and mPEG as the shell. Introduction of biphenyl fragments as hydrophobic spacers near the hPG core substantially increased the hydrophobic guest encapsulation efficiency of the resulting system. The diameter of the nanocarriers was around 50 nm as an aggregate and increased upon interaction with the guest species.<sup>25</sup> The unimolecular micelle-like transport mechanism has also been reported. This nanocarrier system consists of a hPG shell grafted from a dendritic polyethylene core.<sup>26</sup> However, these amphiphilic nanocarrier systems were non-biodegradable.

Chemo-enzymatic modifications on hPGs have been explored leading to amphiphilic polymeric architectures with easily hydrolyzable ester linkages, PEG blocks and alkyl chains. These architectures were used to encapsulate Nile red. The release of Nile red from these polymers was observed with a half-life time of 8 hours at pH 5.0, while no release was found at pH 7.4.<sup>27</sup>

Despite these initial results for molecular transport systems based on hPGs, further studies are required to better understand the mechanism of molecular transport (unimolecular *versus* micelle or aggregate), the influence of the polarity gradient between the core and the shell, and the interactions between guest molecules and nanocarriers. A systematic study of the effects of core topology, flexibility, and shell composition on the overall transport effectiveness of core–shell nanostructures will provide new insights into this still open question.

Here we report the synthesis of a bi-functional nanocarrier system based on amphiphilic hyperbranched polyglycerol (hPG). Hydrophobic aromatic groups and hydrophilic groups were introduced to the core and the shell through “selective chemical differentiation” and chemo-enzymatic reaction strategies, respectively. The nanocarrier system transports hydrophobic dyes by both polymeric and unimolecular micelle mechanisms. Hydrophobic guest molecules such as pyrene were encapsulated in the hydrophobic core of modified hPG *via* hydrophobic interactions as well as  $\pi$ – $\pi$  stacking, resulting in a unimolecular micelle. A second guest molecule, which has a higher affinity to the shell such as Nile red, was solubilized in the outer shell of the host molecule, connecting the host molecules to form aggregates. Furthermore, different controlled release profiles of encapsulated dyes under acid conditions and in the presence of enzyme were observed.

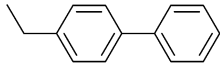
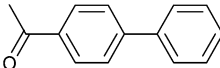
## Results and discussion

### Synthesis of amphiphilic core–shell modified hPG

hPG with a molecular weight ( $M_n$ ) of 5000 g mol<sup>−1</sup> was prepared by anionic ring-opening polymerization of glycidol from deprotonated trimethylolpropane using potassium *tert*-butoxide.<sup>9,28</sup> Post-polymerization modification was performed to diversify macromolecular architecture. The combination of the “selective chemical differentiation” strategy<sup>22</sup> and chemo-enzymatic reaction strategy<sup>29</sup> was used to create three different core–shell nanoparticles based on the hPG scaffold (Table 1 and Scheme 1).

In contrast to dendrimers that contain reactive functionalities only in the shell, *i.e.*, terminal units, additional linear units in hyperbranched polymers are present throughout the structure and can be used for further functionalization. Although randomly incorporated, when the polymers are prepared by slow monomer addition, the linear units will predominate in the proximity of the “core” unit of the macromolecule. A “chemical differentiation” strategy allows a selective modification of the linear units in the “core” of hPG that incorporates the new functional groups. These can be modified independently of the “shell” functionality. In order to distinguish between linear and terminal units, the terminal 1,2-diol groups

**Table 1** Physical characteristics of the core-shell functionalized hPG derivatives<sup>a</sup>

Polymer	-R	-R mol%	mPEG <sub>22</sub> mol%	$M_n \times 10^4$	$M_w/M_n$	$D_h$ nm (DLS)
hPG-A	H	40	30	2.69	1.9	10 <sup>b</sup>
hPG-B		20	30	2.91	1.5	10.8
hPG-C		20	30	2.93	1.4	11.1

<sup>a</sup>  $M_n$  number average molecular weight;  $M_w/M_n$  polydispersity;  $D_h$  mean hydrodynamic diameter. <sup>b</sup> The DLS experiment shows the aggregation as well as small particles of polymer with sizes up to 100 nm, but single particles are around 10 nm.

in the shell were selectively protected with acetone dimethylacetal to yield polyglycerol acetal.<sup>23</sup>

Moreover, a given percentage of the remaining core OH groups were converted into biphenyl ester and biphenyl ether. In the last step, all core functionalized macromolecules were deprotected by treatment with an acidic ionic exchange resin in methanol.<sup>23,24</sup> The core-functionalized hPG-architectures were then pegylated in a regioselective manner by a chemo-enzymatic reaction using the PEG carboxylic acid Novozyme-435 as a biocatalyst.<sup>27,29</sup> The PEG acid was synthesized in a single step from the commercially available PEG monomethyl ether by reacting it with succinic anhydride. The esterification reaction of hPG occurs primarily through the 1° hydroxyl groups of polyglycerol leaving the 2° hydroxyl groups intact (Scheme 1).

Three different core-shell nanocarrier systems were prepared. The core and shell functionality degrees were determined by NMR. The number average molecule weight was obtained by GPC and NMR. The hydrodynamic diameters obtained from dynamic light scattering experiments are listed in Table 1.

### Carrier properties of hPG

**Unimolecular micelle-like carrier properties: solubilization of pyrene.** Pyrene was used as a model drug to get information about the microenvironment and binding sites of the drug delivery system. For the encapsulation experiments of pyrene, a 2 mM pyrene solution was freshly prepared by dissolving an appropriate amount of the dye in dry THF. Aliquots (200  $\mu$ L) were then added to 2 mL of the aqueous polymer solutions with various concentrations in Milli-Q water. After subsequent removal of the organic solvent, the obtained aqueous solutions were stirred for at least 18 h at room temperature. The mixture was filtered through a syringe filter (Rotilabo, 0.45  $\mu$ m pore size) to remove the insoluble excess of pyrene.

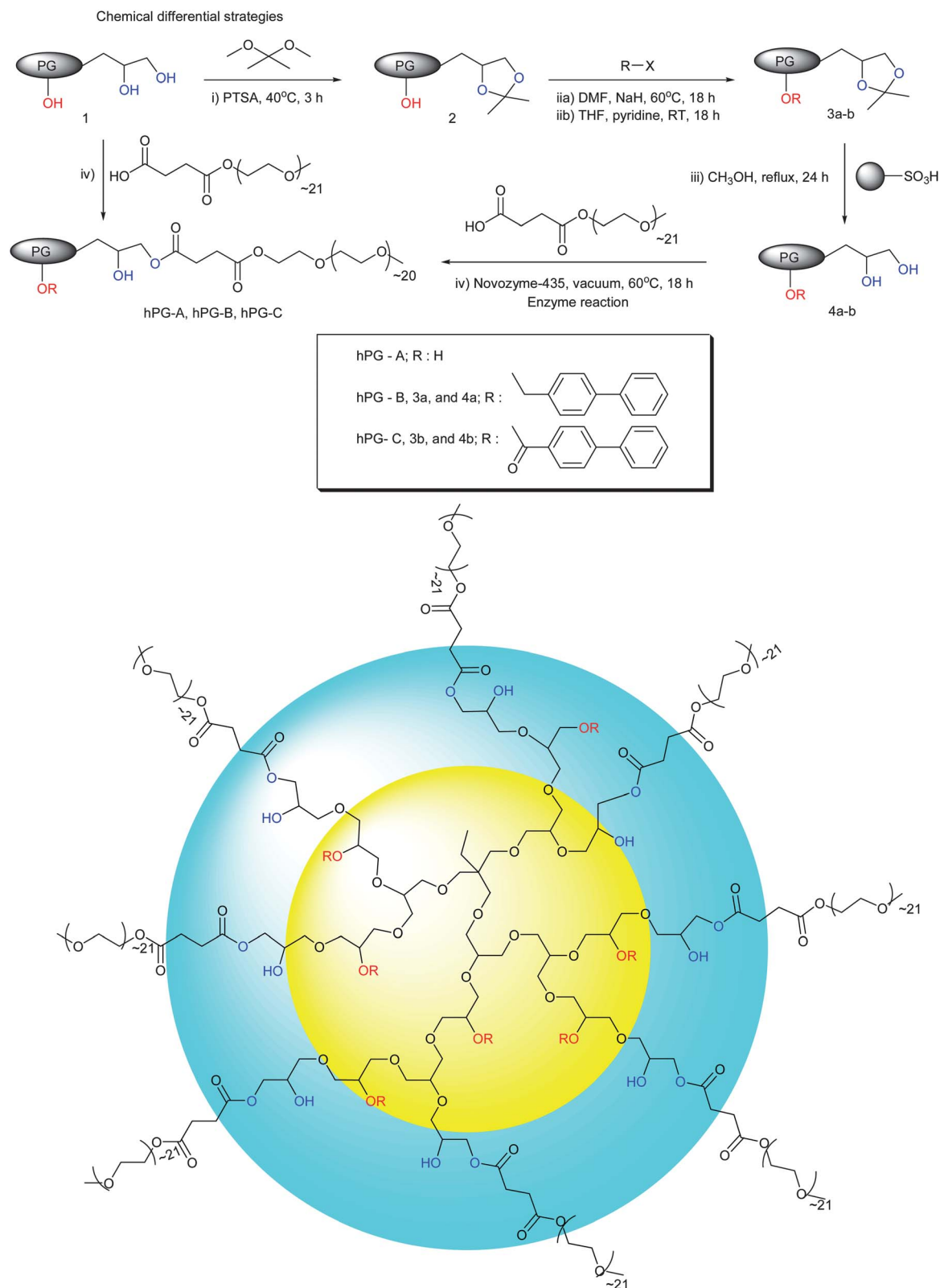
Fig. 1 demonstrates absorbance spectra of pyrene encapsulated at different concentrations of hPG-C. A linear dependence of pyrene absorbance on the polymer concentration was obtained. From the absorbance data, the encapsulated pyrene concentration was calculated. At a polymer concentration of 0.75 mg mL<sup>-1</sup>, an average of 1.4 mol pyrene was encapsulated in one mol polymer hPG-C and 2.0 mol pyrene was encapsulated in one mol polymer hPG-B (ESI†).

The diameter of the polymer was around 10 nm (Table 1). No significant changes in size were observed after pyrene was encapsulated, which was confirmed by DLS and AFM results (Fig. 5 and Table 2). Both findings support the suggestion that the polymer encapsulated pyrene is a unimolecular nanocarrier.

The polarity index of pyrene ( $I_3/I_1$ , the ratio of the intensities of the third (384 nm) and first (372 nm) vibronic peaks in the emission spectrum) can be used as an indicator of the hydrophobicity of the environment in which the pyrene is located.<sup>30</sup> The fluorescence spectroscopy study indicated that the  $I_3/I_1$  ratios of pyrene in hPG-B and hPG-C were 1.02 and 0.97, respectively (ESI†). These values were significantly larger than those of ethylene glycol (0.63) and methanol (0.75), which have a similar composition to the PG shell. Similar results (1.08) were reported for hPG with a polyethylene core.<sup>26</sup> Therefore we conclude that pyrene was encapsulated in the hydrophobic core of hPG by a “unimolecular micelle-type” mechanism.

**Polymeric micelle carrier properties: solubilization of Nile red.** To determine the transport capacity properties of the polymeric scaffolds in buffered aqueous solution Nile red dye was used as a solvatochromic (lipophilic) guest molecule.<sup>31</sup> For the encapsulation experiments, a 20 mM Nile red stock solution was freshly prepared by dissolving an appropriate amount of the dye in dry THF. Aliquots (5–200  $\mu$ L) were then added to 5 mL of the aqueous polymer solutions (5 mg mL<sup>-1</sup>) in Milli-Q water, and after subsequent removal of the organic solvent, the obtained aqueous solutions were stirred for at least 18 h at room temperature. The mixture was filtered through a syringe filter (Rotilabo, 0.45  $\mu$ m pore size) to remove the insoluble excess of Nile red. The aqueous solutions of the polymers were then analyzed by means of UV-Vis and fluorescence spectroscopy.

Fig. 2a presents typical UV-Vis spectra of Nile red-loaded hPG-C in water. At low amounts of the dye (5 and 10  $\mu$ L), a single broad peak around 570 nm was observed. In general, absorbance increases with an increasing amount of Nile red added to the system within the experimental concentration range with vibrations between 30  $\mu$ L and 50  $\mu$ L (Fig. 2a). At amounts higher than 20  $\mu$ L an additional growing peak around 670 nm was observed, with an increasing amount of Nile red. For example, from 20  $\mu$ L to 30  $\mu$ L, the extra peak remains almost the same; while from 30  $\mu$ L to 40  $\mu$ L, it doubles its height and stays constant up to 60  $\mu$ L (Fig. 2a). A shoulder peak around 510 nm



**Scheme 1** Two strategies for making a core-shell nanotransport system: (a) chemical differential strategies ((i)–(iii)) and (b) enzyme reaction (iv).

becomes obvious to the eye after 60  $\mu\text{L}$  and dominates from 100  $\mu\text{L}$ . Fig. 2b shows the corresponding fluorescence emission spectra of dye-loaded hPG-C polymers excited at 550 nm. Within

the experimental concentration range, all emission curves exhibit single broad peaks with a peak maximum around 630 nm, which slightly shift to longer wavelengths with a rising

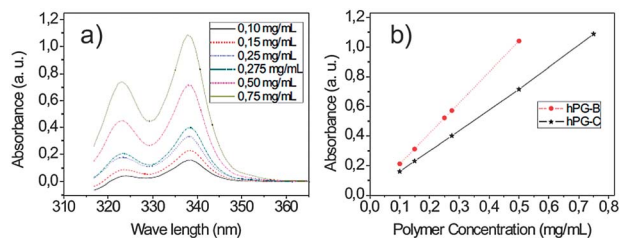


**Fig. 1** (a) UV-Vis spectra of pyrene loaded hPG-C and (b) linear dependence of loaded pyrene on the polymer concentration: hPG-B (circle) and hPG-C (star).

amount of Nile red, *e.g.*, from 626 nm at 5  $\mu\text{L}$  to 636 nm at 200  $\mu\text{L}$  (Fig. 2b). Similar to the absorbance in excitation spectra, the fluorescence intensity rises from 5  $\mu\text{L}$  to 30  $\mu\text{L}$  and oscillates between 30  $\mu\text{L}$  and 50  $\mu\text{L}$ . It reaches the maximum intensity at 60  $\mu\text{L}$  and then drops, saturating after 100  $\mu\text{L}$ .

In order to separate the three peaks in UV-Vis spectra, a 3-peak Gaussian fitting is used. All curves from 20  $\mu\text{L}$  to 200  $\mu\text{L}$  are fitted (Fig. 3a–d). The three peaks are shown by blue dotted lines. Details of the peaks are listed in Table 2 (ESI†). Fig. 3e demonstrates the variation of emission intensity between 5  $\mu\text{L}$  and 200  $\mu\text{L}$  (square) as well as the peak height ratio between peak two to peak three. The fluorescence intensity profile shows a similar variation pattern to the peak ratio, which reflects the ratio of monomer to J-aggregate in the solution.

Nile red has been extensively used as a probe molecule for solvent polarity and hydrophobicity. Due to its solvatochromic behavior, the absorption and emission maxima strongly depend on the polarity of the environment.<sup>32</sup> From the spectroscopic results, absorption maxima between 558 nm and 566 nm as well as emission maxima between 626 nm and 636 nm were observed (Fig. 3). These values fit well with the absorption maxima of Nile red in a mixture of 60 wt% of dioxane in water ( $\lambda_{\text{max}} = 559 \text{ nm}$ ,  $\epsilon = 40.9$ ), respectively, as well as in ethylene glycol ( $\lambda_{\text{max}} = 557 \text{ nm}$ ). By looking carefully at the core-shell structure of the host molecule, one can infer that Nile red preferably resides within the outer layer of the host molecule, where the local polarity is close to that of ethanol and ethylene glycol. The peak in the lower wavelength regions appears to be around 510 nm for the H-aggregate and the peak is around 670 nm for the J-aggregate of Nile red.

In aqueous solution Nile red-modified 2-deoxyuridine has been shown to self-assemble into left-handed helically twisted H-type aggregates.<sup>33</sup> An unusual hypsochromic shift has been assigned to  $\pi$ - $\pi$  interactions between the aromatic dye

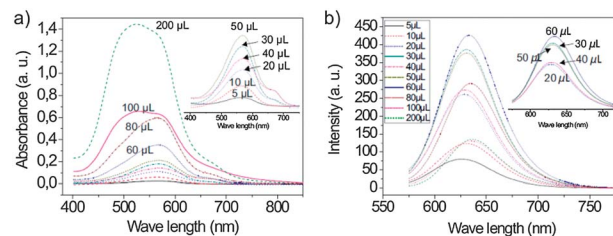


**Fig. 2** (a) UV-Vis spectra and (b) fluorescence spectra of Nile red-loaded hPG-C in water.

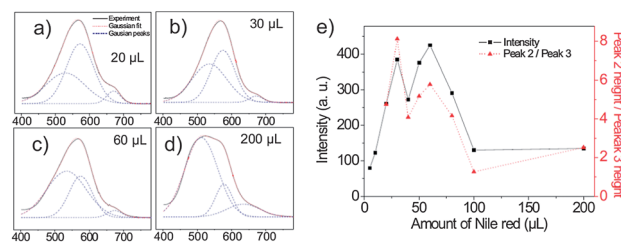


**Fig. 3** Gaussian fitting of the excitation curves at (a) 20  $\mu\text{L}$ , (b) 30  $\mu\text{L}$ , (c) 60  $\mu\text{L}$ , and (d) 200  $\mu\text{L}$  together with (e) variation of emission intensity (square) as well as the ratio of Peak 2 to Peak 3.

molecules in combination with hydrogen bonding ability of the nucleoside and sugar moieties. Similar observations by our group support the formation of H-aggregates of Nile red in aqueous solution.<sup>34</sup> As shown for a series of sugar based polymers, Nile red tends to form dye-polymer (dye) aggregates, in accordance with an unusual hypsochromic shift in aqueous media.

The formation of dye aggregate is also supported by examining the changes of fluorescence on the Nile red concentration. The excitation was carried out at 550 nm, which is mainly the monomer absorption region. Since the absorption band of the J-aggregate overlaps with the emission band of the monomer and the J-aggregate is the main fluorescence quench factor, the fluorescence intensity depends on the ratio of monomer to J-aggregate. A similar dependence of fluorescence and monomer to J-aggregate ratio on the Nile red concentration (Fig. 3e) soundly confirms the co-existence of Nile red monomer and aggregate in the system. The formation of Nile red aggregate is further supported by DLS and AFM size examination experiments (Fig. 5). In summary, we conclude that Nile red resides in the outer shell of hPG, connecting hPG molecules to form

**Table 2** Polymer loading capacity

Polymer	Solubility of Nile red <sup>a,b</sup>	Solubility of pyrene <sup>a</sup>	$I_3/I_1$ in pyrene fluorescence spectra	$D_h$ pyrene-loaded polymer <sup>c</sup>	$D_h$ Nile red-loaded polymer <sup>c</sup>
hPG-A	$6.8 \times 10^{-4}$	—	0.58	—	215
hPG-B	$7.1 \times 10^{-3}$	2.0	1.02	12	184
hPG-C	$7.7 \times 10^{-3}$	1.4	0.97	11	191

<sup>a</sup> Moles of dye per mole of polymer. <sup>b</sup> The maximum concentration of Nile red monomer binding in polymer. <sup>c</sup>  $D_h$ : mean hydrodynamic diameter from DLS experiment in nm.

aggregates. By controlling the amount of the Nile red (to avoid the H- or J-type Nile red aggregates) the loading capacity of the nanocarrier systems was calculated and is listed in Table 2. Note that the values are not the maximum Nile red loadings but only the loading of the Nile red monomer (Nile red aggregates are not included).

**Co-carrier properties: simultaneous solubilization of pyrene and Nile red.** To understand the nanocarrier-guest and guest-guest interactions, the polymer hPG-C was co-loaded with both pyrene and Nile red. First, pyrene was encapsulated into the nanocarrier systems and a 2 mM pyrene solution was freshly prepared by dissolving an appropriate amount of the dye in dry THF. Aliquots (50  $\mu\text{L}$ ) were then added to 5 mL of the aqueous polymer solutions (5  $\text{mg mL}^{-1}$ ) in Milli-Q water after subsequent removal of the organic solvent and the obtained aqueous solutions were stirred for at least 18 h at room temperature. The mixture was filtered through a syringe filter (Rotilabo, 0.45  $\mu\text{m}$  pore size) to remove the insoluble excess of pyrene. 10  $\mu\text{L}$  Nile red aliquot solution was added to the pyrene-polymer solution after subsequent removal of the organic solvents. The obtained aqueous solutions were stirred for at least 18 h at room temperature. The mixture was filtered through a syringe filter (Rotilabo, 0.45  $\mu\text{m}$  pore size) to remove the insoluble excess of Nile red.

By comparing the UV-Vis (Fig. 4) and fluorescence spectroscopy (ESI†) of co-encapsulated pyrene and Nile red with only pyrene or Nile red encapsulated in the polymer, one may see that the intensity and peak maxima of pyrene and Nile red remained unchanged. This result implies that there is no strong interaction between two guest molecules, which confirms our hypothesis that pyrene stays in the core of the hPG while Nile red is located in the outer shell.

**Characterization of guest-nanocarrier complex by AFM and DLS.** AFM experiments were performed to gain a deeper insight into nanocarrier-guest interaction. The pure nanocarrier existed as single particles with a diameter of around 10 nm on the surface (Fig. 5a), which fits well with the DLS results (Table 1).

We attribute the single particles to single polymer molecules. A similar size (11 nm) was obtained from DLS experiments.

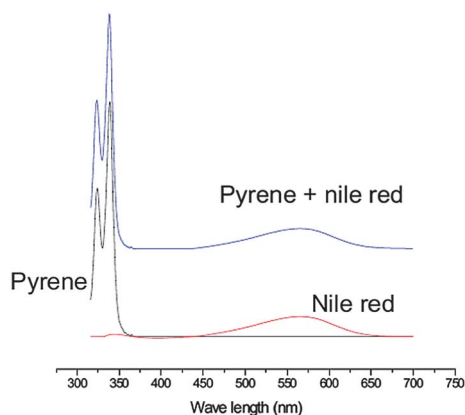


Fig. 4 UV absorbance spectroscopy of co-loaded Nile red and pyrene in hPG-C.

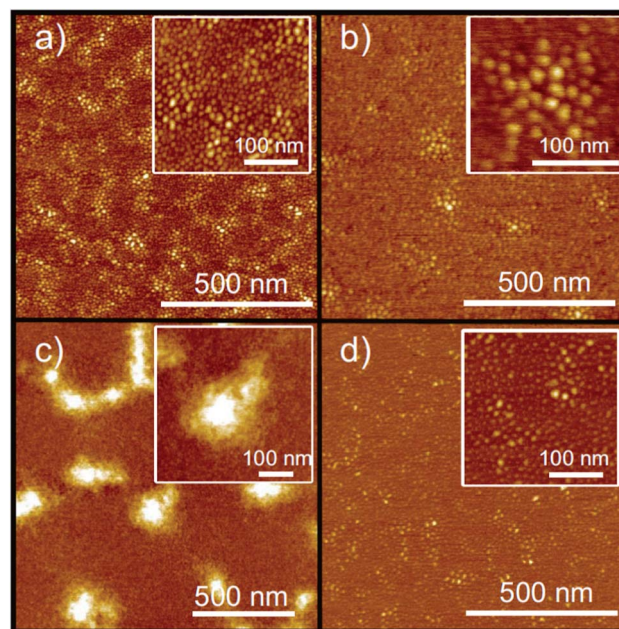


Fig. 5 AFM height images of (a) 0.1  $\text{mg mL}^{-1}$  hPG-C, (b) 0.1  $\text{mg mL}^{-1}$  hPG-C loaded with pyrene, (c) 0.1  $\text{mg mL}^{-1}$  hPG-C loaded with Nile red, and (d) 0.02  $\text{mg mL}^{-1}$  hPG-C loaded with Nile red.

Pyrene is located inside the core of the polymer, which led to an insignificant change in the size of the polymer-pyrene complex compared with a pure polymer. This is confirmed by a similar size distribution from AFM and DLS results. On the other hand, Nile red tends to locate in the outer shell of the polymer, connecting polymer molecules, which leads to the formation of large aggregates (100–200 nm). The Nile red-polymer complexes were not stable and fell apart by dilution.

#### Guest molecule release study

**Release of Nile red under acidic conditions.** We studied the time dependent release of solubilized Nile red at acidic pH (100 mM, pH 5.0, 37  $^{\circ}\text{C}$ ) by means of fluorescence spectroscopy. Experiments were performed to investigate the derivative hPG polymer. We pursued the protocols described by Gillies *et al.* in 2004.<sup>35</sup> The polymers were first equilibrated with Nile red overnight in 10 mM phosphate buffer (pH 7.4). The solution was divided into two samples. The pH of one sample was adjusted to 5.0 by addition of a small aliquot of concentrated acetate buffer (4 M). The second sample was maintained at pH 7.4 but the salt concentration was adjusted to the same as that of the previous sample, which was 100 mM, by addition of concentrated phosphate buffer (2 M) to exclude any effect due to changes of salt concentration.

Fig. 6a presents the fluorescence spectra of Nile red-loaded hPG-C in an acidic solution of pH 5.0 at different time intervals. The maximum intensity decreased exponentially with time at pH 5.0 while no significant changes were observed at pH 7.4 (Fig. 6b). From the data a half-life time of 38.2 and 38.0 hours for hPG-B and hPG-C was obtained at pH 5.0 respectively. A complete release was observed after one week.

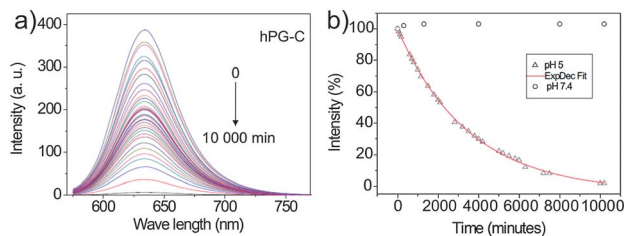


**Fig. 6** (a) Fluorescence intensity curves observed at different time intervals during release of Nile red from hPG-C and (b) maximum fluorescence intensity observed at different time intervals in buffered solution of pH 5.0 (triangle) and pH 7.4 (circles) at 37 °C.

Compared with a previous result, the half time of the polymer was much longer,<sup>27</sup> in other words, the polymer degraded slowly. To confirm the degradability of the polymer under acidic conditions, DLS experiments were performed. The DLS results showed a significant decrease in diameter from around 200 nm before Nile red was released to 9.5 nm after Nile red was completely released (which is similar to the size of the pure polymer). The *in vitro* release of guest molecules under acidic conditions makes the polymer a potential candidate for drug delivery and release in an acidic environment, such as skin, inflammation, and tumor tissue.

We also performed release experiments for the pyrene-loaded polymer using the same protocol. Contrary to the Nile red as a guest molecule, pyrene did not show release in the acidic solution at pH 5.0 within 2 weeks of observation.

To confirm the degradability of the polymer under acidic conditions an *in vitro* aqueous degradation study was performed. The experiment was done under the same conditions already described by Brooks *et al.*<sup>17</sup> The polymer hPG-C was dissolved in buffer solutions of pH 5 (30 mM acetate buffer with 70 mM NaNO<sub>3</sub>) at a concentration of 10 mg mL<sup>-1</sup> and incubated at 37 °C. Samples were withdrawn at 10 days and 27 days and analyzed by size exclusion chromatography for molecular weight characteristics of the polymer. A decrease in molecular weight was detected after 10 and 27 days (Fig. 7).

The average molecular weight decreased from 29 to 17 K. The hPG core was reported earlier to be stable under similar conditions.<sup>16</sup> Therefore we attribute the decrease in molecule weight to the cleavage of PEG chains.<sup>36</sup> The degradation of the nanocarrier leads to the decomposition of the host-guest complex aggregates, which was confirmed by the changes in particle size as observed by DLS. The DLS results showed a significant decrease in diameter from around 200 nm to 9.5 nm. Nile red was thus released during the decomposition of the aggregates while pyrene stayed unaffected. This explains the different release profiles of Nile red and pyrene and is consistent with our hypothesis that the Nile red is located in the PEG shell while pyrene in the core.

**Release of pyrene with enzyme.** Since the hPG derivative polymer contained succinic anhydride as a linker and some of the polymer contained an ester bond in the core, the enzymatic breakdown was investigated. The hydrophobic guest molecules pyrene and Nile red were used for monitoring the degradation of

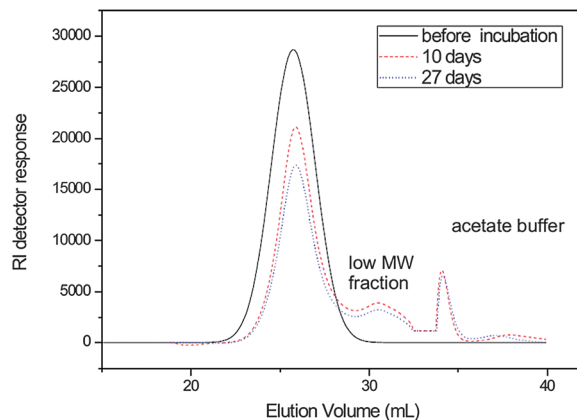


**Fig. 7** Time-dependent GPC chromatograms of hPG-C after incubation in buffer solution of pH 5.0 at 37 °C.

the polymer. Enzyme mediated cleavage was performed with a general de-esterification method using *Candida Antarctica Lipase b.*<sup>37,38</sup> Initially all Nile red or pyrene guest molecules were encapsulated in a sample of the dendritic polymer in PBS buffer (phosphate buffered saline, 10 mM, pH 7.4, 2 mL). After removing the insoluble excess of the dye by filtering the sample through a syringe filter (Rotilabo, 0.45 μm pore size), a few drops of *n*-butanol were added into the aqueous solution. Finally, the enzyme (200 wt% of wt dendritic polymer) was added to the solution. The reaction mixture was stirred at 37 °C for 4 weeks. The experiment was monitored from time to time and checked by fluorescence spectroscopy.

Fig. 8 presents the exponential decay of fluorescence intensity maximum of pyrene-loaded hPG-C in the presence of enzyme with a half time of 6.6 days. A complete release of pyrene was observed after 28 days. The  $I_3/I_1$  ratio was reduced from 1.02 to 0.58. In contrast, for hPG-B the fluorescence intensity was reduced to only 70% of its initial intensity after 28 days. The  $I_3/I_1$  ratio reduced from 0.97 to 0.81. In contrast, in the absence of enzyme no significant decay was observed for hPG-B and hPG-C. When we performed the experiments with Nile red as a

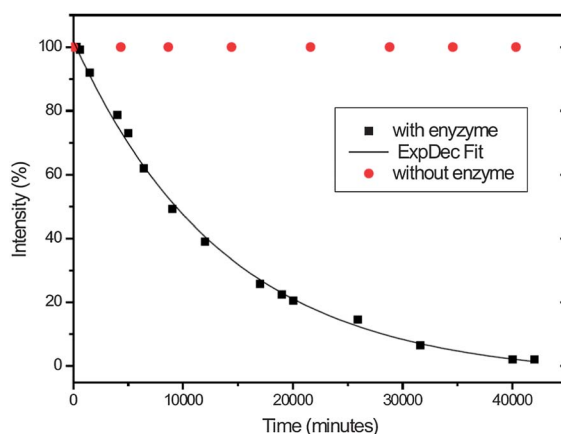


**Fig. 8** Fluorescence intensity decay of pyrene-loaded hPG-C with and without enzyme at 37 °C.

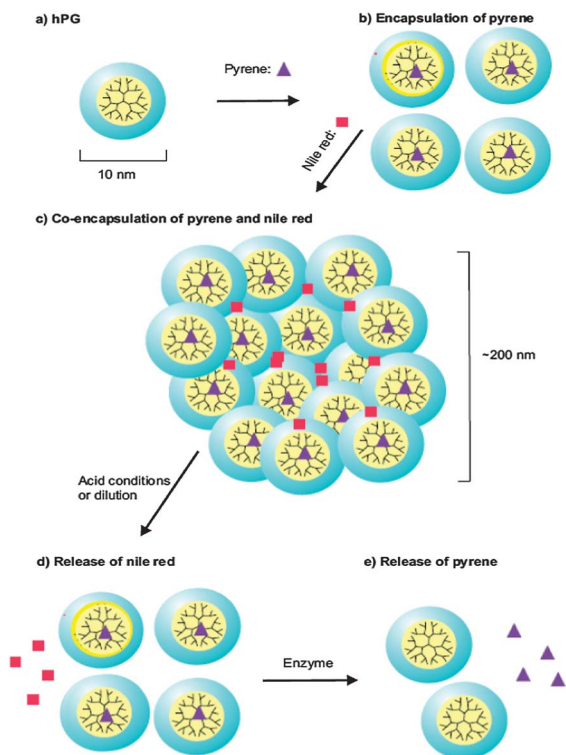


**Fig. 9** Encapsulation and release mechanism: (a) single polymer ca. 10 nm, (b) encapsulation of pyrene by a unimolecular mechanism, (c) co-encapsulation of two guest molecules, (d) release of Nile red under acid conditions, and (e) release of pyrene in the presence of an enzyme.

guest molecule, the fluorescence intensity maximum was reduced to 67% of its initial intensity after 28 days.

In hPG-C the aromatic moieties are linked to the core by ester bonds, while in hPG-B they are linked by ether bonds. The enzyme we used reacted selectively with ester bonds in hPG-C and therefore removed the hydrophobic aromatic moieties from the core of hPG-C, which caused the release of pyrene.

## Conclusion and outlook

In summary, we have synthesized a bi-functional nanocarrier system based on a dendritic hyperbranched polyglycerol (hPG) structure, which contains hydrophobic groups in the core and hydrophilic groups in the shell. The polymer solubilized and released pyrene and Nile red by different mechanisms. Pyrene is encapsulated in the core of the polymer, which reveals the unimolecular micelle type carrier properties of the polymer. No release of pyrene was observed upon dilution or under acid conditions in this case. The release of encapsulated pyrene was only achieved in the presence of enzyme, which selectively cleaved the biphenylesters in the core of the polymer. On the other hand, Nile red was solubilized in the polymer aggregates and the aggregates broke down into single molecules upon dilution, which indicates polymeric micelle-like transport properties. The release of Nile red was achieved at pH 5 (Fig. 9). The different encapsulation mechanisms and controlled release profiles make this polymer a promising candidate for

simultaneous delivery of two hydrophobic drugs, which is a current need for combination therapy, e.g., in cancer treatment.

## Acknowledgements

This work was supported in part by the Focus Area Nanoscale of the Freie Universität Berlin (<http://www.nanoscale.fu-berlin.de>) and the Deutsche Forschungsgemeinschaft.

## Notes and references

- 1 R. Haag and F. Kratz, *Angew. Chem., Int. Ed.*, 2006, **45**, 1198.
- 2 Y. Matsumura and H. Maeda, *Cancer Res.*, 1986, **46**, 6387.
- 3 P. Alexandridis, J. F. Holzwarth and T. A. Hatton, *Macromolecules*, 1994, **27**, 2414.
- 4 A. V. Kabanov, E. V. Batrakova and V. Y. Alakhov, *J. Controlled Release*, 2002, **82**, 189.
- 5 S. Danson, D. Ferry, V. Alakhov, J. Margison, D. Kerr, D. Jowle, M. Brampton, G. Halbert and M. Ranson, *Br. J. Cancer*, 2004, **90**, 2085.
- 6 J. W. Valle, A. Armstrong, C. Newman, V. Alakhov, G. Pietrzynski, J. Brewer, S. Campbell, P. Corrie, E. K. Rowinsky and M. Ranson, *Invest. New Drugs*, 2011, **29**, 1029.
- 7 D. Astruc, E. Boisselier and C. Ornelas, *Chem. Rev.*, 2010, **110**, 1857.
- 8 R. Haag, *Chem.-Eur. J.*, 2001, **7**, 327.
- 9 A. Sunder, R. Mulhaupt, R. Haag and H. Frey, *Adv. Mater.*, 2000, **12**, 235.
- 10 H. Frey and R. Haag, *J. Biotechnol.*, 2002, **90**, 257.
- 11 M. Calderon, M. A. Quadir, S. K. Sharma and R. Haag, *Adv. Mater.*, 2010, **22**, 190.
- 12 S. Reichert, P. Welker, M. Calderon, J. Khandare, D. Mangoldt, K. Licha, R. K. Kainthan, D. E. Brooks and R. Haag, *Small*, 2011, **7**, 820.
- 13 J. Khandare, A. Mohr, M. Calderon, P. Welker, K. Licha and R. Haag, *Biomaterials*, 2010, **31**, 4268.
- 14 R. Wilson, B. J. Van Schie and D. Howes, *Food Chem. Toxicol.*, 1998, **36**, 711.
- 15 D. Howes, R. Wilson and C. T. James, *Food Chem. Toxicol.*, 1998, **36**, 719.
- 16 R. K. Kainthan, M. Gnanamani, M. Ganguli, T. Ghosh, D. E. Brooks, S. Maiti and J. N. Kizhakkedathu, *Biomaterials*, 2006, **27**, 5377.
- 17 R. K. Kainthan and D. E. Brooks, *Bioconjugate Chem.*, 2008, **19**, 2231.
- 18 C. Kojima, K. Yoshimura, A. Harada, Y. Sakanishi and K. Kono, *J. Polym. Sci., Part A: Polym. Chem.*, 2010, **48**, 4047.
- 19 R. K. Kainthan, C. Mugabe, H. M. Burt and D. E. Brooks, *Biomacromolecules*, 2008, **9**, 886.
- 20 F. Wurm, J. Klos, H. J. Raeder and H. Frey, *J. Am. Chem. Soc.*, 2009, **131**, 7954.
- 21 L. A. Tziveleka, C. Kontoyianni, Z. Sideratou, D. Tsiourvas and C. M. Paleos, *Macromol. Biosci.*, 2006, **6**, 161.
- 22 R. Haag, J. F. Stumbe, A. Sunder, H. Frey and A. Hebel, *Macromolecules*, 2000, **33**, 8158.

- 23 H. Tuerk, A. Shukla, P. C. A. Rodrigues, H. Rehage and R. Haag, *Chem.–Eur. J.*, 2007, **13**, 4187.
- 24 I. N. Kurniasih, H. Liang, J. P. Rabe and R. Haag, *Macromol. Rapid Commun.*, 2010, **31**, 1516.
- 25 I. N. Kurniasih, H. Liang, V. D. Moeschwitzer, M. A. Quadir, M. Radowski, J. P. Rabe and R. Haag, *New J. Chem.*, 2012, **36**, 371.
- 26 C. S. Popeney, M. C. Lukowiak, C. Boettcher, B. Schade, P. Welker, D. Mangoldt, G. Gunkel, Z. Guan and R. Haag, *ACS Macro Lett.*, 2012, **1**, 564.
- 27 S. Kumar, A. Mohr, A. Kumar, S. K. Sharma and R. Haag, *Int. J. Artif. Organs*, 2011, **34**, 84.
- 28 A. Sunder, R. Hanselmann, H. Frey and R. Mulhaupt, *Macromolecules*, 1999, **32**, 4240.
- 29 S. Gupta, M. K. Pandey, K. Levon, R. Haag, A. C. Watterson, V. S. Parmar and S. K. Sharma, *Macromol. Chem. Phys.*, 2010, **211**, 239.
- 30 K. Kalyanasundaram and J. K. Thomas, *J. Am. Chem. Soc.*, 1977, **99**, 2039.
- 31 A. Y. Jee, S. Park, H. Kwon and M. Lee, *Chem. Phys. Lett.*, 2009, **477**, 112.
- 32 J. Jose and K. Burgess, *Tetrahedron*, 2006, **62**, 11021.
- 33 R. Varghese and H. A. Wagenknecht, *Chem.–Eur. J.*, 2010, **16**, 9040.
- 34 S. Bhatia, A. Mohr, D. Mathur, V. S. Parmar, R. Haag and A. K. Prasad, *Biomacromolecules*, 2011, **12**, 3487.
- 35 E. R. Gillies, T. B. Jonsson and J. M. J. Frechet, *J. Am. Chem. Soc.*, 2004, **126**, 11936.
- 36 E. R. Gillies, E. Dy, J. M. Frechet and F. C. Szoka, *Mol. Pharm.*, 2005, **2**, 129.
- 37 N. B. Bashir, S. J. Phythian, A. J. Reason and S. M. Roberts, *J. Chem. Soc., Perkin Trans. 1*, 1995, 2203.
- 38 J. Mauricio Mora-Pale, S. Perez-Munguia, J. C. Gonzalez-Mejia, J. S. Dordick and E. Barzana, *Biotechnol. Bioeng.*, 2007, **98**, 535.
- 39 I. Göss, L. Shu, A. D. Schlüter and J. P. Rabe, *J. Am. Chem. Soc.*, 2002, **124**, 6860.
- 40 N. Severin, J. Barner, A. Kalachev and J. P. Rabe, *Nano Lett.*, 2004, **4**, 577.
- 41 A. Mohr, T. P. Vila, H.-G. Korth, H. Rehage and R. Sustmann, *ChemPhysChem*, 2008, **9**, 2397.
- 42 A. Mohr, P. Talbiersky, H.-G. Korth, R. Sustmann, R. Boese, D. Bläser and H. Rehage, *J. Phys. Chem. B*, 2007, **111**, 12985.
- 43 M. Almgren, F. Grieser and J. K. Thomas, *J. Am. Chem. Soc.*, 1979, **101**, 279.